

Patterned Condensation Figures as Optical Diffraction Gratings

Amit Kumar and George M. Whitesides*

Patterned Condensation Figures as Optical Diffraction Gratings

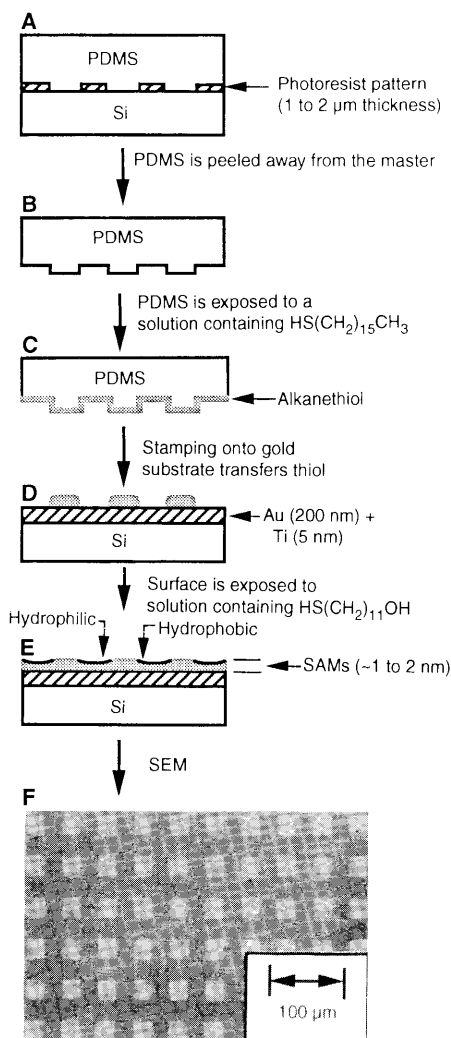
Amit Kumar and George M. Whitesides*

Heterogeneous, patterned surfaces comprising well-defined hydrophobic and hydrophilic regions and having micrometer-scale periodicities were prepared by patterning the adsorption of ω -functionalized alkanethiolates in self-assembled monolayers (SAMs) on gold. Condensation of water on such surfaces resulted in drops that followed the patterns in the SAMs. These patterned condensation figures (CFs) acted as optical diffraction gratings for reflected (or transmitted) light from a helium-neon laser (wavelength of 632.8 nanometers). Under an atmosphere of constant relative humidity, the development of the condensation figure was monitored quantitatively, as the temperature of the surface was lowered, by following the change in intensity of a first-order diffraction spot. This experimental technique may be useful in the development of new types of optical sensors that respond to their environment by changing the reflectivity of patterned regions and for studying phenomena such as drop nucleation, contact angle hysteresis, and spontaneous dewetting and break-up of thin liquid films.

Condensation figures (CFs) are arrays of liquid drops that form upon condensation of vapor onto a solid surface (1, 2). The examination of condensation figures has historically been used as a method to characterize the degree of contamination on an otherwise homogeneous surface (1). We have been able to impose a pattern on arrays of condensed drops by patterning the surface underlying them into regions of different solid-vapor interfacial free energy and have characterized the patterned CFs by photomicroscopy (3). Here we demonstrate that appropriately patterned CFs can be used as optical diffraction gratings and that examination of the diffraction patterns provides both a rapid, nondestructive method for characterizing them and an approach to sensing their environment. Because the form of the CFs—that is, the size, density, and distribution of the drops—is sensitive to environmental factors, CFs of appropriate size and pattern diffract light and can be used as sensors. We demonstrate this principle by correlating the temperature of a substrate patterned into hydrophobic and hydrophilic regions, in an atmosphere of constant relative humidity, with the intensity of light diffracted from CFs on these regions.

Appropriate patterns were formed from self-assembled monolayers (SAMs) on gold by using combinations of hexadecanethiol [$\text{CH}_3(\text{CH}_2)_{15}\text{SH}$], 16-mercaptohexadecanoic acid [$\text{HS}(\text{CH}_2)_{15}\text{COOH}$], and 11-mercaptoundecanol [$\text{HS}(\text{CH}_2)_{11}\text{OH}$]. Several techniques are now available for preparing patterns of two or more SAMs having 0.1- to 10- μm dimensions (4–6). Here we used a polydimethylsiloxane (PDMS)

stamp, replicated from a photolithographically patterned polymethylmethacrylate master, to transfer thiols to the surface of gold (4, 7). The procedure for the preparation of the patterned surface and a scanning



electron micrograph (SEM) of a representative pattern are shown in Fig. 1.

The extent of formation of CFs as a function of the temperature of the surface in contact with moist air is shown in Fig. 2. At 20°C, an incident beam of light from a laser (helium-neon laser, wavelength = 632.8 nm) produced a single reflected spot because no water had condensed on the surface, and the reflectivity of the regions covered with different SAMs were effectively indistinguishable. As the temperature of the surface was lowered, droplets of water formed on it; these droplets initially formed preferentially on the hydrophilic regions. Diffraction patterns appeared in the light reflected from the surface. Under these conditions, light was reflected coherently from the regions where no water had condensed and was scattered by the regions where water had condensed. As the temperature of the surface was decreased further, enough water condensed on the surface to begin bridging the hydrophilic regions; the periodicity of the pattern changed, and the diffraction began to weaken. When bridging was extensive or com-

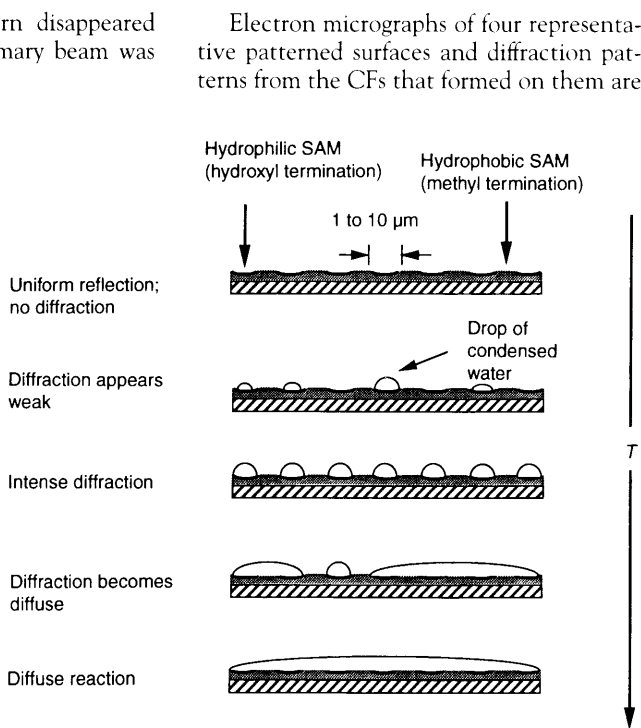
Fig. 1. Procedure for fabrication of elastomeric stamp and preparation of patterned surface (4). Features are not drawn to scale. (A) An exposed and developed photoresist pattern on a silicon wafer was used as the master. Polydimethylsiloxane (PDMS; Silicone Elastomer 184, Dow Corning Corp., Midland, Michigan) was polymerized on the master and carefully peeled away (B). (C) The stamp was inked by exposure to a solution (1 to 10 mM in ethanol) of one alkanethiol; the PDMS areas that were brought into contact with the ink swelled slightly. (D) The inked stamp was brought into contact with the gold substrate and removed. (E) The substrate was washed for 2 to 4 s with a solution of a second alkanethiol (1 to 10 mM in ethanol). The substrate was finally washed for 10 s with ethanol and dried in a stream of nitrogen. In (E), the regions of the SAMs containing hydrophobic groups are indicated schematically by a dark line and the regions containing $-\text{CH}_3$ groups by gray shading. (F) This electron micrograph is representative of a patterned surface (8). A stamp having square features, 25 μm on a side, was used to pattern $\text{HS}(\text{CH}_2)_{15}\text{CH}_3$ (light regions) on the gold; the gold was subsequently exposed to $\text{HS}(\text{CH}_2)_{11}\text{OH}$ (dark regions).

Department of Chemistry, Harvard University, Cambridge, MA 02138.

*To whom correspondence should be addressed.

plete, the diffraction pattern disappeared and reflection from the primary beam was also diffused by scattering.

Fig. 2. Schematic representation of the formation of condensation figures. In the absence of condensation, the incident laser beam is reflected as a single beam. As the temperature (T) of the surface is lowered, water from the air condenses on the surface. Condensation progresses from a few nonuniform droplets on some of the hydrophilic regions to uniform droplets that cover all of the hydrophilic regions. A diffraction pattern appears as the CFs form coherent patterns, and becomes more intense as the hydrophilic regions become uniformly covered with water. Eventually, bridging occurs between adjacent droplets and the diffraction pattern weakens and disappears.



In the SEMs shown in Fig. 3, A to C, the dark regions are SAMs terminated with carboxylic acid groups and the light regions are SAMs terminated with methyl groups. A pattern formed from regions of methyl-terminated, carboxyl-terminated, and hydroxyl-terminated SAMs is shown in Fig. 3D (8).

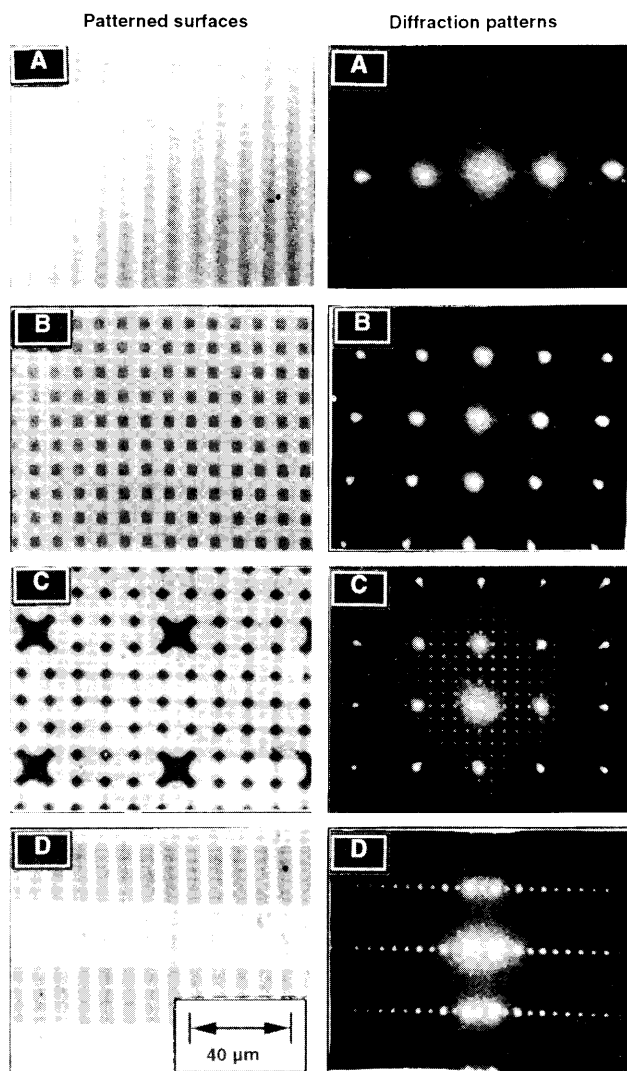
The surface in Fig. 3A was formed with a stamp consisting of parallel lines to imprint a pattern of $\text{HS}(\text{CH}_2)_{15}\text{CH}_3$. The surface in Fig. 3B was formed with the same stamp as that for the pattern in Fig. 3A by imprinting the surface twice with the stamp rotated by 90° between imprints. The pattern of Fig. 3C was formed by imprinting once with a stamp consisting of two different lattices. Figure 3D underscores the utility of the rubber stamping technique for the formation of patterns with more than two SAMs. The grid was formed by first stamping parallel lines with $\text{HS}(\text{CH}_2)_{15}\text{CH}_3$, and then a series of parallel lines with $\text{HS}(\text{CH}_2)_{11}\text{OH}$ with a different stamp. The two series of parallel lines had different periodicities and different orientations. The background was derivatized by exposure of the substrate to $\text{HS}(\text{CH}_2)_{15}\text{CO}_2\text{H}$.

The diffraction patterns observed from the patterned SAMs in Fig. 3 are those expected from a reflective surface covered with nonreflective drops whose shapes replicate those of the underlying hydrophilic SAMs. The diffraction patterns were photographed when the surfaces were at a temperature that produced the most intense diffraction.

The diffraction patterns from Fig. 3, A and B, are straightforward, whereas the diffraction patterns from Fig. 3, C and D, are more complex. The pattern of Fig. 3C has two periodicities in surface patterning: a lattice of small features with a small spacing and a lattice of larger features with a larger spacing. The diffraction patterns from these two lattices are clearly separated in Fig. 3C. This type of separation offers the opportunity to examine the comparative rates of formation of condensation drops on areas of different size, shape, and in principle surface composition by using one as a reference for the other. The pattern of Fig. 3D has two lattices of different periodicity, orientation, and composition. The two independent diffraction patterns (Fig. 3D) are distinguishable by orientation and lattice spacing. By varying these parameters, it should be possible to place a number of independent diffracting elements on a common surface.

Quantitative measurements of the intensities of the diffraction spots were useful in determining the properties of the environment and progression of condensation. The pattern shown in Fig. 3A was placed on a brass stage whose temperature could be varied under an atmosphere of controlled relative humidity. The sam-

Fig. 3. Electron micrographs of patterned surfaces (left) and diffraction patterns from CF formed on these surfaces (right). (A) A SAM comprising lines of $\text{HS}(\text{CH}_2)_{15}\text{CH}_3$ (light) in a field of a SAM formed from $\text{HS}(\text{CH}_2)_{15}\text{CO}_2\text{H}$ (dark), and diffraction of a helium-neon laser beam ($\lambda = 632.8 \text{ nm}$, 1 mW) from a CF formed on this surface. (B) A grid formed by stamping $\text{HS}(\text{CH}_2)_{15}\text{CH}_3$ (light) followed by exposure of the surface to $\text{HS}(\text{CH}_2)_{15}\text{CO}_2\text{H}$ (dark), and the corresponding diffraction pattern. (C) The diffraction patterns of surfaces with more than one periodicity are distinguishable. (D) A surface having three patterned SAMs and corresponding diffraction pattern. In this pattern, vertical, light lines are $-\text{S}(\text{CH}_2)_{15}\text{CH}_3$; horizontal, light lines are $-\text{S}(\text{CH}_2)_{11}-\text{OH}$; and the dark background is $-\text{S}(\text{CH}_2)_{15}\text{CO}_2\text{H}$. The preparation of the surface and the corresponding diffraction pattern are described in the text.



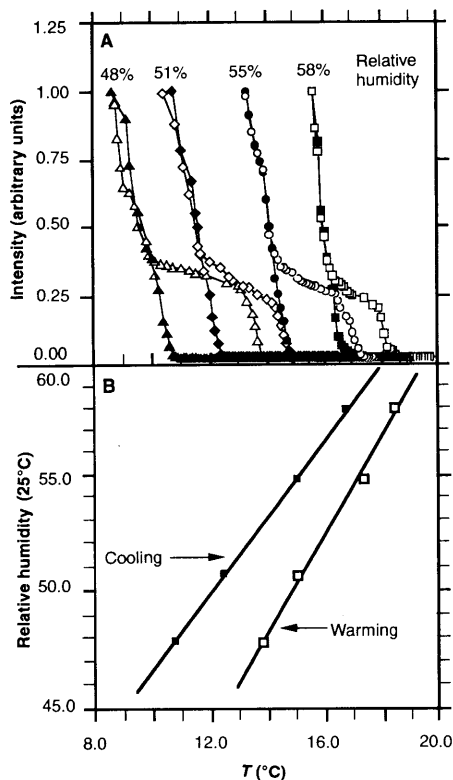


Fig. 4. (A) Plot of intensity of a first-order diffraction spot as a function of temperature T of the surface. Under atmospheres of different relative humidities, the surface shown in Fig. 3A was cooled or warmed, and the intensity of a first-order diffraction spot was monitored with a UDT-Silicon photodiode (United Detector Technologies, Irvine, California). The solid points were measured as the sample was cooled (0.5° to 1°C per second), and the open points were measured as the sample was warmed (1° to 2°C per second). (B) The intercepts on the T axis of lines fit to the rising and falling portions of the curves shown in (A) are linearly related to the relative humidity.

ple was cooled or warmed, and its temperature was monitored with a thermocouple. The quantitative change in intensity as a function of sample temperature for a first-order diffraction spot under atmospheres of different relative humidities is depicted in Fig. 4A (9). In all cases, as the temperature of the surface decreased, there was initially a slow rise in intensity (not visible in Fig. 4A), followed by a rapid rise. As the sample was cooled further, the water droplets began to bridge across the hydrophobic regions, and a decrease in intensity was observed (not shown). The warming curves exhibited significant hysteresis from the cooling curves. This hysteresis may be due to several factors. During cooling, the surface temperature must be low enough for nucleation of droplets to occur. During warming, the dewetting process is dependent on factors such as the local humidity near the surface and the surface-to-volume ratio of the drops as their size changes. In

addition, advancing and receding contact angle measurements on surfaces of SAMs exhibit considerable hysteresis, reflecting the different factors that control wetting and dewetting (10).

Figure 4B shows linear relations between relative humidity (over the range from 48 to 58% at 25°C) and the intercept on the temperature axis for a line fit through the rapidly rising portion of the cooling curves and the rapidly decreasing portion of the warming curves. These data demonstrate that diffraction from these systems of patterned SAMs is very sensitive to relative humidity and suggest the use of these systems as sensors for humidity and other environmental factors. In addition to diffraction in a reflective geometry, these systems also produce diffraction in a transmission geometry. The use of semitransparent, thin (100 to 300 Å) gold films, deposited on glass slides (11), allowed diffraction from condensation figures to be observed for incident beams that were transmitted through the condensation figure.

These studies demonstrate the utility of regularly patterned SAMs as diffracting systems with which to analyze and use CFs. The ability to change the size, shape, and chemical composition of multiple arrays of spots simultaneously and independently, and to study the diffraction of light from them as a function of properties—the vapor pressure of condensable vapors, temperature, and concentrations of materials that might adsorb from solution or suspension—of the environment surrounding the surface that influence their reflectivity make these systems highly flexible tools with which to

study phenomena in surface science (12). Their versatility, and the ability to use optical methods for assay, may provide advantages in designing sensors that are not practical with other techniques. In addition, this very sensitive method of characterizing CFs will be useful in studying the process of nucleation and formation and breakup of thin films.

REFERENCES AND NOTES

1. Lord Rayleigh, *Nature* **86**, 416 (1911); J. Aitken, *ibid.*, p. 516; Lord Rayleigh, *ibid.* **90**, 436 (1912); R. Merigoux, *Rev. Opt.* **9**, 281 (1937).
2. C. M. Knobler, *Physica A* **140**, 198 (1986); D. Beysens and C. M. Knobler, *Phys. Rev. Lett.* **57**, 1433 (1986); F. Perrot and D. Beysens, *Rev. Sci. Instrum.* **58**, 183 (1987); B. J. Briscoe and K. P. Galvin, *Colloids Surf.* **56**, 263 (1991).
3. G. P. López, H. A. Biebuyck, C. D. Frisbie, G. M. Whitesides, *Science* **260**, 647 (1993).
4. A. Kumar and G. M. Whitesides, *Appl. Phys. Lett.* **63**, 2002 (1993).
5. A. Kumar, H. A. Biebuyck, N. L. Abbott, G. M. Whitesides, *J. Am. Chem. Soc.* **119**, 4198 (1992).
6. N. L. Abbott, J. P. Folkers, G. M. Whitesides, *Science* **257**, 1380 (1992).
7. Although the data reported in the work was obtained from alkanethiolate SAMs supported on gold, similar results were obtained for SAMs on copper and silver.
8. G. P. López, H. A. Biebuyck, G. M. Whitesides, *Langmuir* **9**, 1513 (1993).
9. Relative humidity was measured with an analog hygrometer from Fisher Scientific (Pittsburgh, PA).
10. J. P. Folkers, P. E. Laibinis, G. M. Whitesides, *Langmuir* **8**, 1330 (1992).
11. P. A. DeMilla *et al.*, unpublished results.
12. A sensor based on diffraction from patterns of adsorbed proteins has been demonstrated: S. Deshpande and R. M. Rocco, Idetek Corporation, Sunnyvale, CA.
13. Supported in part by the Office of Naval Research, ARPA, and by the National Science Foundation (grant NSF PHY-9312572).

23 September 1993; accepted 8 November 1993